Aging of nickel manganite NTC ceramics

**Dao-lai Fang · Cui-hong Zheng · Chu-sheng Chen ·
A. J. A. Winnubst**

Abstract Effect of thermal history and chemical composition on aging of $Ni_xMn_{3-x}O_{4+\delta}$ ($0.56 \leq x \leq 1.0$) ceramics was investigated. It was found that all the $Ni_xMn_{3-x}O_{4+\delta}$ ceramic samples metallized by co-firing at 1050°C showed significant electrical stability with an aging coefficient less than 1.0%, while aging of those metallized by annealing at 850°C was increasingly serious with a rise in Ni content x, the aging coefficient ranging from 0.2% to 3.8%. However, the ceramic samples with Ni content $x \leq 0.70$, whether metallized by co-firing or by annealing, exhibited extraordinarily high electrical stability with an aging coefficient less than 0.5%. The composition dependence of aging of the ceramic samples was explained qualitatively, based on the electrical conduction mechanism of small polaron hopping and on the aging mechanism of the cationic vacancy-assisted migration of cations to their thermodynamically preferable sites under thermal stress.

Keywords Nickel manganite · Aging · Cation vacancy · Small polaron hopping

D.-l. Fang · C.-s. Chen (✉)
Laboratory of Advanced Functional Materials and Devices,
Department of Materials Science and Engineering,
University of Science and Technology of China,
Hefei, Anhui 230026, People's Republic of China
e-mail: ccsm@ustc.edu.cn

D.-l. Fang · C.-h. Zheng
School of Materials Science and Engineering,
Anhui Key Laboratory of Metal Materials and Processing,
Anhui University of Technology,
Ma'anshan, Anhui 243002, People's Republic of China

A. J. A. Winnubst
Inorganic Materials Science,
MESA + Institute of Nanotechnology, University of Twente,
P.O. Box 217, 7500 AE Enschede, The Netherlands

1 Introduction

As a kind of the technologically important semiconducting materials for negative temperature coefficient (NTC) thermistors, spinel nickel manganite ceramics have been extensively investigated, involving their preparation, microstructure, cation distribution and electrical properties [1–4]. It is widely accepted that cation distribution of $Ni_xMn_{3-x}O_4$ is expressed as $\left(Ni^{2+}_{x(1-\alpha)}Mn^{2+}_{1-x(1-\alpha)} \right) \left[Ni^{2+}_{\alpha x}Mn^{3+}_{2-2\alpha x}Mn\ \alpha x^{4+} \right]O_4$, in which the parentheses denote the tetrahedral sites, the square brackets the octahedral sites, α the inversion parameter of Ni^{2+} cations [2, 4]. The electrical conduction mechanism of the spinel manganites is elaborated to be the small polaron hopping model, namely, a phonon-assisted hopping of charge carriers between Mn^{3+} and Mn^{4+} cations in the octahedral sites of spinel [5].

However, there exists much controversy on aging of the nickel manganite ceramics. Fritsch et al. [2] found that almost no aging was observed in $Ni_{0.73}Mn_{2.27}O_4$ ceramic thermistors metallized in nitrogen, while aging of those metallized in air was considerably serious, suggesting that the oxidation of the ceramics occurring during metallization was responsible for the aging phenomena. But Groen et al. [6] reported that $Ni_{0.54}Mn_{2.46}O_4$ ceramic thermistors metallized in air exhibited significant electrical stability with an aging coefficient less than 0.5%. Furthermore, Metz et al. [7] claimed that aging of tetragonally distorted $Ni_xMn_{3-x}O_4$ ceramics with lower Ni content was more serious on the basis of his proposed aging mechanism that aging originated from formation of Mn^{3+} clustering in the octahedral sites. In a word, it is not quite clear that how thermal history and composition affect aging of the nickel manganite ceramic thermistors.

The partial oxidation of $Ni_xMn_{3-x}O_{4+\delta}$ ceramic samples, usually occurring during preparation and subsequent

annealing for electrode curing, can be characterized by the oxygen non-stoichiometry δ formed. However, due to the minuteness of the oxygen non-stoichiometry δ of $Ni_xMn_{3-x}O_{4+\delta}$ ceramics, there still exists a great difficulty in determining the accurate value of δ by thermogravimetry. In this paper, chemical analysis was attempted to determine the accurate value of δ, and effect of thermal history and composition on aging of the $Ni_xMn_{3-x}O_{4+\delta}$ ($0.56 \le x \le 1.0$) was investigated. The possible aging mechanisms operating were proposed to explain the aging phenomena in the ceramic samples.

2 Experimental procedure

2.1 Preparation of the ceramic samples

The mixed nickel manganese oxalate precursors for $Ni_xMn_{3-x}O_{4+\delta}$ ($x=0.56, 0.66, 0.76, 0.82, 1.0$) oxide powders were prepared by the route of solid-state coordination reaction, which was described in detail in our previous work [1]. The mixed oxide powders were obtained by calcining the mixed oxalate precursors at 850°C for 2 h. The oxide powders were uniaxially pressed at 60 MPa to form disk-shaped samples with a diameter of ~6 mm and a thickness of ~3 mm, and then isostatically pressed at 300 MPa. The powder compacts were sintered at 1050°C for 5 h in air, subsequently cooled in furnace.

For electrical measurement, the electrodes have to be placed on the two opposite surfaces of the obtained ceramic disks, using two different methods of metallization. The classic method, usually used in industry, called 'serigraphy', includes brushing the platinum paste on the two surfaces of the disks, and annealing the disks at 850°C for 20 min, followed by rapid cooling to room temperature. The other method is called co-firing, including brushing platinum paste on the two opposite surfaces of the powder compacts, sintering in air the pasted compacts at 1050°C for 5 h, followed by rapid cooling to room temperature. The thermistor samples can be obtained by attaching Ag wires to these metallized ceramic samples.

2.2 Determination of chemical compositions and oxygen non-stoichiometry δ

The accurate contents of Ni and Mn ions in the resulting ceramics were determined by chemical analysis, which was described in our previous work [1]. The method for determination of the oxygen non-stoichiometry δ of $Ni_xMn_{3-x}O_{4+\delta}$ ceramic samples is elucidated in brief as follows:

The powdered ceramic samples are dissolved in an $(NH_4)_2Fe(SO_4)_2$ solution of known Fe^{2+} content in hydro-

chloric acid, using a closed vessel with an inert atmosphere of nitrogen. As a powerful oxidant, Mn^{3+} and Mn^{4+} ions in solution oxidize Fe^{2+} ions into Fe^{3+} ions. According to the formula $Ni_x^{2+}Mn_{3-x}^zO_{4+\delta}$, the oxidation equivalents $k = z - 2 = \frac{2+2\delta}{3-x}$ (z is the average oxidation number of Mn) will be transferred to Fe^{2+} ions yielding Fe^{3+} ions, and can be determined by titrating the residual Fe^{2+} ion concentration using a $K_2Cr_2O_7$ solution of known Cr^{6+} molarity as the standard solution, sodium diphenylamine sulfonate as indicator. Thus δ value can be calculated on the basis of the principle of electroneutrality. The standard deviation of δ is estimated to be ±0.004.

2.3 Analysis of phase compositions and electrical measurement

A Philips X'pert Pro X-ray diffractometer with $Cu_{K\alpha}$ radiation ($\lambda = 1.5418$ Å) was used to analyze the phase compositions of the sintered ceramics. The bulk density ρ_{bulk} of the ceramic samples was determined by Archimedes method in mercury, and their relative density ρ_{rel} was calculated from the formula $\rho_{rel} = \rho_{bulk}/\rho_{th}$, where ρ_{th} was the theoretical density as obtained from XRD data of ceramic samples.

The thermistor samples' resistance at 25°C was measured with an Agilent 34401A digital multimeter, during which the thermistor samples were immersed in silicon oil whose temperature fluctuation around the designating value was less than ±0.05°C. The aging coefficient is characterized by the relative variation $[(R_{1,000\ h} - R_0)/R_0] \times 100\%$, in which R_0 is the resistance value measured at 25°C before annealing, $R_{1,000\ h}$ is the resistance value measured at 25°C after annealing at 150°C for 1,000 h.

3 Results and discussion

3.1 Chemical and phase compositions of the 1050°C-sintered ceramics

The actual chemical compositions of the 1050°C-sintered ceramics, prepared by the solid-state coordination reaction route, are determined by chemical analysis, as given in Table 1. The results show the ceramic samples are very close to the desired nominal $Ni_xMn_{3-x}O_{4+\delta}$ ($x=0.56, 0.66, 0.76, 0.82, 1.0$). The relative density of all the ceramic samples is measured to be ~97%. The accurate composition and high density of the resulting ceramics are beneficial to improvement of the reproducibility and reliability of the samples' electrical parameters measured.

Figure 1 is X-ray diffraction patterns of the 1050°C-sintered $Ni_xMn_{3-x}O_{4+\delta}$ ($x=0.56, 0.66, 0.76, 0.82, 1.0$) ceramic samples. As shown in Fig. 1(a, b, c, d), the samples

Table 1 Oxygen non-stoichiometry δ in 2 batches of $Ni_xMn_{3-x}O_{4+\delta}$ (x=0.56, 0.66, 0.76, 0.82, 1.0) ceramic samples metallized by co-firing and 850°C-annealing.

| Chemical compositions	Co-sintered samples δ ($\pm$0.004)	Annealed samples δ ($\pm$0.004)	NiO content (wt.%)
$Ni_{0.562}Mn_{2.438}O_{4+\delta}$	$Ni_{0.562}Mn_{2.438}O_{4.004}$	$Ni_{0.562}Mn_{2.438}O_{4.045}$	0
$Ni_{0.657}Mn_{2.343}O_{4+\delta}$	$Ni_{0.657}Mn_{2.343}O_{3.999}$	$Ni_{0.657}Mn_{2.343}O_{4.026}$	0
$Ni_{0.762}Mn_{2.238}O_{4+\delta}$	$Ni_{0.762}Mn_{2.238}O_{4.001}$	$Ni_{0.762}Mn_{2.238}O_{4.023}$	0
$Ni_{0.823}Mn_{2.177}O_{4+\delta}$	$Ni_{0.823}Mn_{2.177}O_{3.988}$	$Ni_{0.823}Mn_{2.177}O_{4.028}$	0
$Ni_{0.995}Mn_{2.005}O_{4+\delta}$	$Ni_{0.995}Mn_{2.005}O_{3.934}$	$Ni_{0.995}Mn_{2.005}O_{4.000}$	6.39
	$(0.198NiO + 0.934Ni_{0.859}Mn_{2.141}O_{4.000})$	$(0.198NiO + 0.934Ni_{0.859}Mn_{2.141}O_{4.071})$	

of intermediate Ni content x=0.66, 0.76, 0.82 retain single cubic spinel, while the sample with lower Ni content x=0.56 is transformed to tetragonal spinel due to the high concentration of the B-site Mn^{3+} ions, which arouse a strong Jahn–Teller effect, consequently the tetragonal distortion in the octahedral sublattices. However, as indicated in Fig. 1(e), the (222), (400) and (440) peaks of the $Ni_xMn_{3-x}O_{4+\delta}$ (x=1.0) sample broaden evidently, implying a slight amount of rocksalt NiO is formed due to the decomposition of the spinel at 1050°C, in accordance with Wickham's report that $NiMn_2O_{4+\delta}$ starts to decompose at a temperature above 950°C [8].

3.2 Oxygen non-stoichiometry δ of $Ni_xMn_{3-x}O_{4+\delta}$ ceramic samples

The oxygen non-stoichiometry δ of two batches of $Ni_xMn_{3-x}O_{4+\delta}$ (x=0.56, 0.66, 0.76, 0.82, 1.0) ceramic samples, metallized by co-firing at 1050°C and by annealing at 850°C, respectively, is given in Table 1.
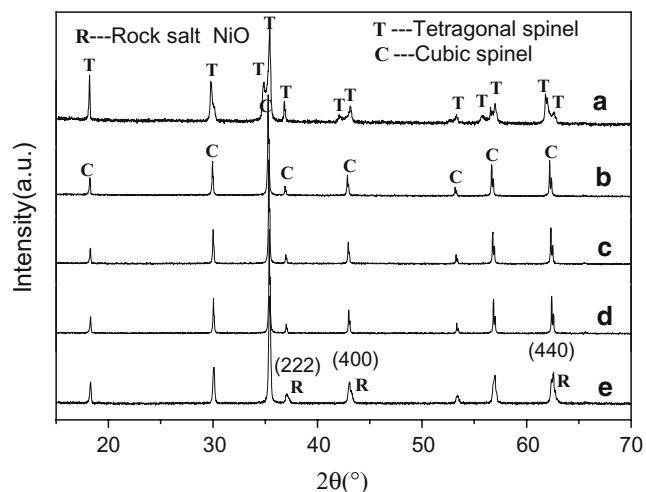
As for the $Ni_xMn_{3-x}O_{4+\delta}$ samples metallized by co-firing, the samples with lower Ni content x=0.56, 0.66, 0.76 almost

Fig. 1 X-ray diffraction patterns of the $Ni_xMn_{3-x}O_{4+\delta}$ ceramic samples subjected to co-firing at 1050°C. (*a*) x=0.56; (*b*) x=0.66; (*c*) x=0.76; (*d*) x=0.82; (*e*) x=1.0

retain the correct oxygen stoichiometry with $\delta \approx 0$, but those with higher Ni content x=0.82, 1.0 deviate evidently from the correct oxygen stoichiometry with $\delta < 0$. However, the evident loss of oxygen ($\delta < 0$) of the sample with a nominal chemical formula of $NiMn_2O_{4+\delta}$ is attributed to the release of oxygen during its decomposition at a temperature higher than 950°C:

$$NiMn_2O_4 \rightarrow aNiO + \frac{3-a}{3}Ni_{\frac{3-3a}{3-a}}Mn_{\frac{6}{3-a}}O_4 + \frac{a}{6}O_2 \quad (1)$$
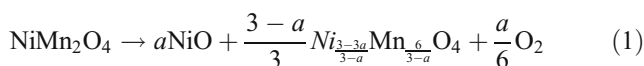
Due to the release of oxygen during the phase decomposition, it is almost impossible that an oxygen non-stoichiometry $\delta < 0$ exists in the residual spinel-structured $Ni_{\frac{3-3a}{3-a}}Mn_{\frac{6}{3-a}}O_{4+\delta}$. Nevertheless, the residual spinel nickel manganite is less likely to become the one with an oxygen non-stoichiometry $\delta > 0$ under a sintering temperature as high as 1050°C [9]. Thus it is reasonable that the residual spinel nickel man-ganite is treated as the one with the correct oxygen stoichiometry $\delta = 0$. On the basis of the the Eq. 1 and the above argument, the $Ni_xMn_{3-x}O_{4+\delta}$ (x=1) ceramic sample, which has been determined to have a nominal chemical formula of $Ni_{0.995}Mn_{2.005}O_{3.934}$, is calculated to be composed of $aNiO + \frac{3-a}{3}Ni_{\frac{3(0.995-a)}{3-a}}Mn_{\frac{3\times2.005}{3-a}}O_4$. Therefore, the '$a$' value, charactering the formed NiO content, can be calculated to be 0.198 by considering the invariance of the total number of oxygen anions. From the obtained 'a' value, the content of the formed rocksalt NiO is calculated to account for 6.39 wt. % of the two-phase ceramics. Due to the formed NiO content just above the detectable threshold of X-ray, its diffraction peaks are less pronounced, as shown in Fig. 1(e).

The $Ni_xMn_{3-x}O_{4+\delta}$ samples metallized by annealing at 850°C have a larger oxygen non-stoichiometry δ than those of the samples metallized by co-firing. The larger δ of the annealed $Ni_{0.56}Mn_{2.44}O_{4+\delta}$ sample can be ascribed to a higher concentration of the octahedral-site Mn^{3+} ions, which are prone to oxidation [10]. The extraordinarily larger δ of the annealed $NiMn_2O_{4+\delta}$ sample may be associated with the reverse reaction of the Eq. 1, e.g. the re-adsorption of NiO and oxygen into the residual nickel-poor spinel during the 850°C-annealing for the electrode curing. As indicated in Fig. 2(b), the diffraction peaks of NiO phase in the 850°C-annealed $Ni_xMn_{3-x}O_{4+\delta}$ (x=1.0)
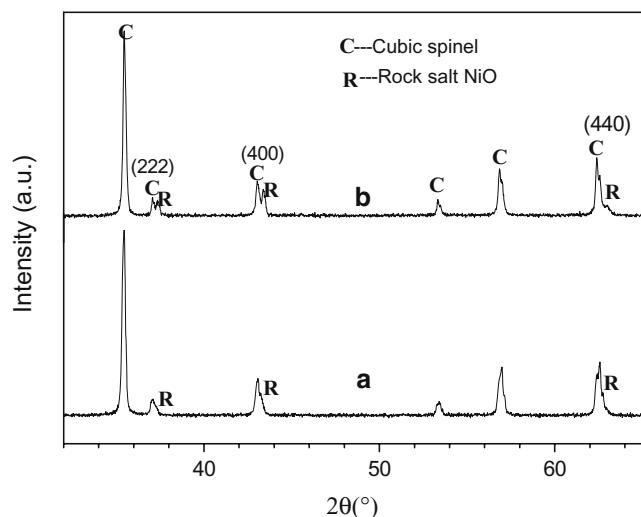
Fig. 2 X-ray diffraction patterns of two kinds of $Ni_xMn_{3-x}O_{4+\delta}$ ($x=$ 1.0) ceramic samples subjected to (a) co-firing at 1050°C; (b) annealing at 850°C

sample become sharper than those of the co-fired sample, implying that the 850°C-annealing results in the growth of the poorly crystallized NiO crystallites formed during sintering at 1050°C. Though the NiO crystallites fails to merge into the nickel-poor spinel in the short duration of 850°C-annealing, it is thermodynamically favored that the oxygen is re-adsorbed into the nickel-poor spinel to form a cation-deficient spinel. Therefore, according to the Eq. 1, it is rational that the nominal spinel-structured $Ni_{0.995}Mn_{2.005}O_{4.000}$ is considered to be actually composed of rocksalt NiO and spinel $Ni_{0.859}Mn_{2.141}O_{4.071}$.

Larson et al. [3] studied the effect of temperature, oxygen partial pressure and Ni content x on the redox in $Ni_{1-x}Mn_{2+x}O_{4+\delta}$ ceramics. It was revealed that under the fixed oxygen partial pressure, a decrease in temperature favors the oxidation of $Ni_{1-x}Mn_{2+x}O_{4+\delta}$ ceramics, resulting in formation of cationic vacancies, while a rise in Ni content facilitates the reduction of the ceramics due to the strong B-site preference of Ni^{2+} cations, leading to formation of oxygen vacancies. As given in Table 1, the oxygen non-stoichiometry δ of the $Ni_xMn_{3-x}O_{4+\delta}$ ($x=0.56$, 0.66, 0.76, 0.82, 1.0) ceramic samples, undergoing different thermal history, is well in agreement with Larson's study.
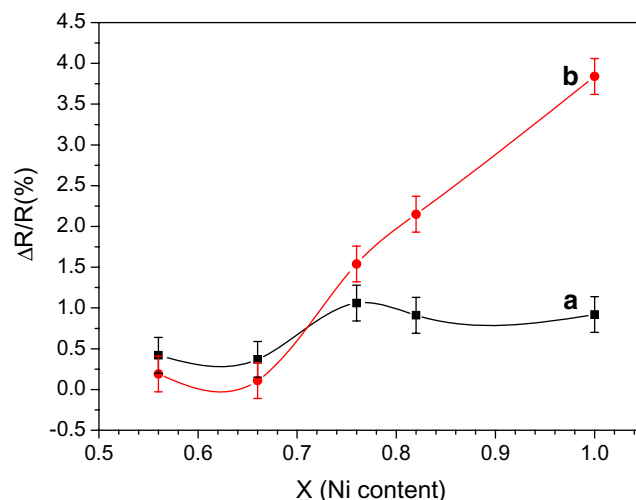
3.3 Aging of the $Ni_xMn_{3-x}O_{4+\delta}$ ceramic samples

3.3.1 Effect of thermal history on the aging

As indicated in Fig. 3, thermal history notably affects aging of the $Ni_xMn_{3-x}O_{4+\delta}$ ceramic samples, especially those with Ni content x higher than 0.70. Aging of all the samples metallized by co-firing is slight with an aging coefficient less than 1.0%, whereas aging of those metallized by an-

nealing at 850°C is considerably serious with the maximum an aging coefficient as high as 3.8%.

In spite of much controversy on aging mechanisms, it is generally accepted that aging of the ceramic samples originates from the migration of cations and cationic vacancies to their thermodynamically preferable sites at an elevated temperature [2, 6, 9, 11]. In general, the migration of cations between the tetrahedral and octahedral sublattices of spinel nickel manganites almost stops at below 350°C due to the high activation energy required [12]. However, in the case of the transition-metal manganite with point defect of cationic vacancies, the situation may be changed, in which the presence of cationic vacancies lowers the activation energy of cation migration, consequently the cation redistribution between spinel sublattices may occur at a lower temperature of ~150°C. In our case, the more serious aging of the 850°C-metallized $Ni_xMn_{3-x}O_{4+\delta}$ samples may be related to the presence of cationic vacancies, which assist the migration of cations to their thermodynamically preferable sublattices at low temperatures, resulting in the pronounced change of the resistivity. Concerning the co-fired $Ni_xMn_{3-x}O_{4+\delta}$ samples, due to almost no cationic vacancies formed during preparation and metallization, it is less possible that the migration of cations occurs at a lower temperature of ~150°C, consequently aging of the samples is very slight. Our results are well in accordance with those of Fritsch et al. [2], who found that almost no aging is observed in $Ni_{0.73}Mn_{2.27}O_4$ sample metallized in nitrogen, while aging of that metallized in air is much larger.

Nevertheless, thermal history hardly affects aging of the samples with Ni content x less than 0.70, as demonstrated in Fig. 3. The possible reasons will be discussed in the following section.

Fig. 3 Variation of aging coefficient of the $Ni_xMn_{3-x}O_{4+\delta}$ ceramic samples with Ni content x and thermal history (a) co-firing at 1050°C; (b) annealing at 850°C

T---Tetragonal spinel   R---Rock salt NiO   C---Cubic spinel
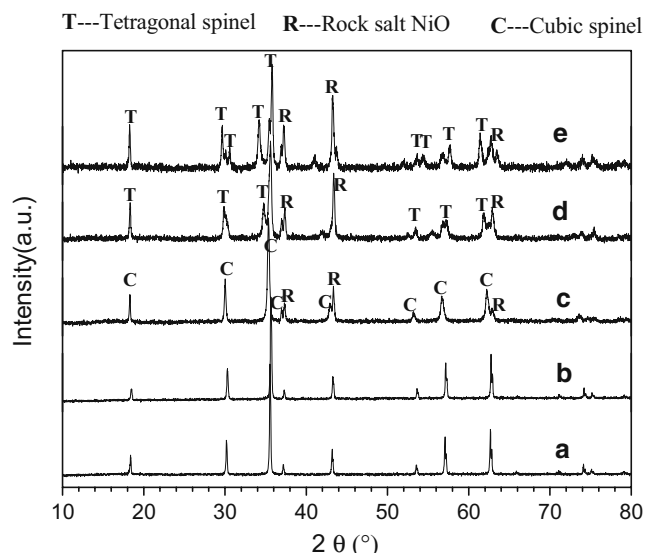
Fig. 4 X-ray diffraction patterns of $NiMn_2O_{4+\delta}$ samples sintered at (a) 1000°C; (b) 1050°C; (c) 1100°C; (d) 1200°C; (e) 1250°C

3.3.2 Composition dependence of aging

Aging of the 850°C-annealed $Ni_xMn_{3-x}O_{4+\delta}$ samples strongly depends on their compositions, as shown in Fig. 3(a). Aging coefficient of the samples with Ni content x less than 0.70 is as small as ~0.2%, while that of the samples with Ni content $x>0.70$ is considerably larger, increasing from 1.5% to 3.8% with a rise in Ni content x.

Boucher [13] has reported that the cation distribution of $Ni_xMn_{3-x}O_{4+\delta}$, generally expressed as $\left(Ni^{2+}_{x(1-\alpha)}Mn^{2+}_{1-x(1-\alpha)}\right)$ $\left[Ni^{2+}_{\alpha x}Mn^{3+}_{2-2\alpha x}Mn^{4+}_{\alpha x}\right]O_4$, is strongly dependent on the sintering or annealing temperatures and on the subsequent cooling rate, with the inversion parameter α varying from 0.74 for the 950°C-quenched sample to 0.93 for the slowly-cooled sample. In our case, the $Ni_xMn_{3-x}O_{4+\delta}$ samples subjected to rapid cooling from 1050°C or 850°C partially retain the random cation distribution, which is thermodynamically preferable at high temperatures, therefore the inversion parameter α is reasonably believed to be a little larger than that of a quenched sample, 0.74. Consequently, the random cation distribution, energetically unfavorable at the room temperature, has a tendency of transformation to the more ordered cation distribution in order to lower the internal energy in spinel lattice. As discussed in the above section, under the assistance of cationic vacancies, the random distributed cations in spinel will migrate to their thermodynamically preferable sublattices at a lower temperature of ~150°C, resulting in an increase in the inversion parameter α and the consequent drift of resistivity, e.g. the occurrence of the aging. On the basis of this aging mechanism, effect of compositions on aging of the 850°C-metallized $Ni_xMn_{3-x}O_{4+\delta}$ samples is discussed qualitatively.

The electrical conduction mechanism of $Ni_xMn_{3-x}O_{4+\delta}$ manganites is described as a small polaron theory, and the conductivity is given by the equation [3, 5]:

$$\sigma = C_{Mn^{3+}} C_{Mn^{4+}} \frac{16e^2d^2}{\upsilon kT} \nu_0 e^{-E_a/kT} \qquad (2)$$

where $C_{Mn^{3+}}$ and $C_{Mn^{4+}}$ are the respective fraction of Mn^{3+} and Mn^{4+} in B sites ($\sum_i C_{M_i} = 1$, C_{M_i} is the fraction of B-site cation M_i), E_a (thermal constant $B=E_a/k$) the activation energy of carriers hopping, υ the volume of the unit cell, ν_0 the optical phonon frequency, d the hopping distance between the nearest neighbor B-site cations, e, k, T have their usual meanings. According to the cation distribution of $\left(Ni^{2+}_{x(1-\alpha)}Mn^{2+}_{1-x(1-\alpha)}\right)\left[Ni^{2+}_{\alpha x}Mn^{3+}_{2-2\alpha x}Mn^{4+}_{\alpha x}\right]O_4$, the conductivity can be expressed as:

$$\sigma = (2-2\alpha x) \cdot \alpha x \cdot M \qquad (3)$$

where M is a parameter associated with the mobility of charge carriers, α the inversion parameter of Ni^{2+} cations. Provided that the mobility does not change with the slight increase of the inversion parameter α, the resulting drift of the conductivity can be denoted as:

$$\Delta\sigma = \frac{d\sigma}{d(\alpha x)}\Delta(\alpha x) = 2M(1-2\alpha x)\Delta(\alpha x) \qquad (4)$$

From the above Eq. 4 the trend of the drift of σ is derived: (a) when $x=1/2\alpha$, $\Delta\sigma=0$, implying resistivity of the sample with Ni content x around $1/2\alpha$ is almost unchanged with the cation re-distribution, e.g. no aging occurs; (b) when $x>1/2\alpha$, $\Delta\sigma<0$, implying that resistivity of the samples with Ni content $x>1/2\alpha$ increases with the cation re-distribution,
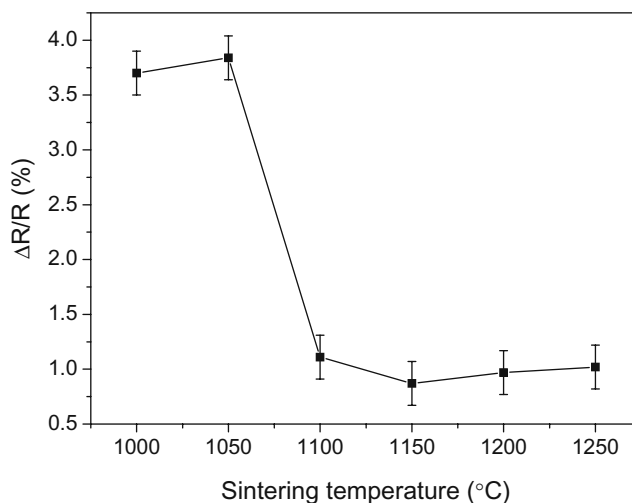
Fig. 5 Sintering temperature dependence of aging of the $NiMn_2O_{4+\delta}$ samples

e.g. the aging occurs; (c) when $x<1/2\alpha$, $\Delta\sigma>0$, implying that resistivity of the samples with Ni content $x<1/2\alpha$ decreases with the cation re-distribution, e.g. aging coefficient is negative. Due to the prepared samples cooled at an intermediate rate between the quenching and the slowly cooling, it is reasonable that the inversion parameter α is set to be an intermediate value of 0.85. Therefore, as for the $Ni_xMn_{3-x}O_{4+\delta}$ samples with x around 0.59, their resistivity changes very slightly with cation re-distribution, but concerning the samples with Ni content x higher than 0.59, the drift of their resistivity becomes increasingly pronounced with a rise in Ni content x.

For the samples metallized by 850°C-annealing, Ni content dependence of aging, as given in Fig. 3(a), is well in accordance with the theoretical results elaborated above, indicating that cation re-distribution over spinel sublattices at an elevated temperature may be a dominant factor responsible for the aging phenomena.

However, the negative aging coefficient predicted has not been observed for the $Ni_xMn_{3-x}O_{4+\delta}$ ($x<0.59$) samples. Aging coefficient of the $Ni_{0.56}Mn_{2.44}O_{4+\delta}$ sample we prepared is as small as 0.2%, which is very consistent with Groen's report that almost no aging is observed for the $Ni_{0.54}Mn_{2.46}O_{4+\delta}$ sample [6]. This implies that there may exist the other secondary aging mechanism working simultaneously. Vandenberghe et al. [11], who studied the oxidation mechanism of spinel copper manganites, found that Mn^{3+} cations in octahedral sites tend to cluster together and orient themselves in order to release the lattice elastic energy in spinel structure. As a result, the probability that a Mn^{3+} cation has a Mn^{4+} cation as its nearest neighbor decreases, resulting in a decrease in the effective concentration of charge carriers, $C_{Mn^{3+}}C_{Mn^{4+}}$, and a consequent increase in resistivity. Metz [7] claimed that formation of Mn^{3+} clustering is a main factor responsible for aging of the transition-metal manganite ceramics. However, in our case, the aging mechanism of formation of Mn^{3+} clustering may play a minor role in the aging phenomena. Slight aging of the $Ni_xMn_{3-x}O_{4+\delta}$ samples with $x\cong0.59$ may be attributed to formation of Mn^{3+} clustering.

3.3.3 Effect of sintering temperatures on aging of $NiMn_2O_{4+\delta}$

The $NiMn_2O_{4+\delta}$ powder compact samples are sintered at temperatures ranging from 1000°C to 1250°C, and the obtained dense ceramic samples are metallized by annealing at 850°C in air, followed by rapid cooling.

X-ray diffraction patterns (Fig. 4) reveal that at a sintering temperature above 1100°C the $NiMn_2O_{4+\delta}$ sample decomposes notably, forming rocksalt NiO and nickel-poor cubic or tetragonal spinel, in accordance with Wickham's results [8]. Because of its high resistivity, the rocksalt NiO does not contribute to the electrical conductivity, thus

hardly affects aging of the samples. It is the nickel-poor cubic or tetragonal spinel that contributes to the electrical conductivity, therefore aging of the $NiMn_2O_{4+\delta}$ ceramic samples is closely related to the electrical properties of the nickel-poor spinel. On the basis of the aging mechanism proposed above, it can be predicted that aging of the $NiMn_2O_{4+\delta}$ ceramic samples sintered at a temperature higher than 1100°C is remarkably alleviated.

As shown in Fig. 5, aging coefficient of the nominal $NiMn_2O_{4+\delta}$ ceramic samples strongly depends on sintering temperatures, decreasing sharply from 3.8% to 1.2% with an elevation of sintering temperature from 1050°C to 1100°C, and holding about 1.0% with a further elevation of sintering temperature. The sintering temperature dependence of aging of the $NiMn_2O_{4+\delta}$ samples is well in agreement with the one predicted above, suggesting the proposed aging mechanism of cation re-distribution over spinel sublattices is reasonable.

4 Conclusion

Aging of $Ni_xMn_{3-x}O_{4+\delta}$ ($0.56\leq x\leq1.0$) ceramic samples strongly depends on their thermal history and compositions. For the samples metallized by co-firing at 1050°C, the correct oxygen stoichiometry is almost retained, and their aging is slight with an aging coefficient less than 1.0%. For the samples metallized by annealing at 850°C, the oxygen non-stoichiometry δ is considerably larger, varying from 0.023 to 0.071, and their aging is increasingly serious with a rise in Ni content x, the aging coefficient increasing from 0.2% to 3.8%. However, the ceramic samples with Ni content $x\leq0.70$, whether metallized by co-firing or by 850°C-annealing, exhibit significant electrical stability with an aging coefficient less than 0.5%. Thermal history and composition dependence of aging of the $Ni_xMn_{3-x}O_{4+\delta}$ ($0.56\leq x\leq1.0$) ceramic samples is explained very well, on the basis of the electrical conduction mechanism of small polaron theory and of the aging mechanism of the cationic vacancy-assisted migration of cations to their thermodynamically preferable sites under thermal stress.

References

1. D.L. Fang, Z.B. Wang, P.H. Yang, W. Liu, C.S. Chen, A.J.A. Winnubst, J. Am. Ceram. Soc. **89**, 230 (2006)
2. S. Fritsch, J. Sarrias, M. Brieu, J.J. Couderc, J.L. Baudour, E. Snoeck, A. Rousset, Solid State Ion. **109**, 229 (1998)
3. E.G. Larson, R.J. Arnott, D.G. Wickham, J. Phys. Chem. Solids **23**, 1771 (1962)
4. B. Gillot, M. Kharroubi, R. Metz, R. Legros, A. Rousset, Solid State Ion. **44**, 275 (1991)

5. I.G. Austin, N.F. Mott, Adv. Phys. **18**, 41 (1969)
6. W.A. Groen, C. Metzmacher, P. Huppertz, S. Schuurman, J. Electroceram. **7**, 77 (2001)
7. R. Metz, J. Mater. Sci. **35**, 4705 (2000)
8. D.G. Wickham, J. Inorg. Nucl. Chem. **26**, 1369 (1963)
9. T. Battault, R. Legros, A. Rousset, J. Mater. Res. **13**, 1238 (1998)
10. C. Drouet, C. Laberty, J.L.G. Fierro, P. Alphonse, A. Rousset, Int. J. Inorg. Mater. **2**, 419 (2000)
11. R.E. Vandenberghe, G.G. Robbrecht, V.A.M. Brabers, Phys. Stat. Sol. A **34**, 583 (1976)
12. V.A.M. Brabers, J.C.J.M. Terhell, Phys. Stat. Sol. A **69**, 325 (1982)
13. B. Boucher, R. Buhl, M. Perrin, Acta Crystallogr. B **25**, 2326 (1969)